J. Serb. Chem. Soc. 67 (5)305-324(2002)
JSCS-2951

UDC 621.357+620.197.5/.6
Review paper

REVIEW

The mechanism of cathodic electrodeposition of epoxy coatings and the corrosion behaviour of the electrodeposited coatings

VESNA B. MIŠKOVIĆ-STANKOVIĆ#

Faculty of Technology and Metallurgy, University of Belgrade, Karnegijeva 4, P. O. Box 3503, YU-11120 Belgrade, Yugoslavia

(Received 17 January 2002)

Abstract. The model of organic film growth on a cathode during electrodeposition process proposes the current density-time and film thickness-time relationships and enables the evaluation of the rate contants for the electrochemical reaction of OH^- ion evolution and for the chemical reaction of organic film deposition. The dependences of film thickness and rate constants on the applied voltage, bath temperature and resin concentration in the electrodeposition bath have also been obtained. The deposition parameters have a great effect on the cathodic electrodeposition process and on the protective properties of the obtained electrodeposited coatings. From the time dependences of the pore resistance, coating capacitance and relative permittivity, obtained from impedance measurements, the effect of applied voltage, bath temperature and resin concentration on the protective properties of electrodeposited coatings has been shown. Using electrochemical impedance spectroscopy, thermogravimetric analysis, gravimetric liquid sorption experiments, differential scanning calorimetry and optical miscroscopy, the corrosion stability of epoxy coatings was investigated. A mechanism for the penetration of electrolyte through an organic coating has been suggested and the shape and dimensions of the conducting macropores have been determined. It was shown that conduction through a coating depends only on the conduction through the macropores, although the quantity of electrolyte in the micropores of the polymer net is about one order of magnitude greater than that inside the conducting macropores.

Keywords: electrodepositon, cathodic electrodeposition, epoxy coatings, corrosion protection, corrosion stability.

CONTENTS

Serbian Chemical Society active member.

1. INTRODUCTION

Electrodeposition of organic coatings has gained worldwide acceptance as a coating process for automotive, appliance and general industrial coatings which has been adopted in technology to provide the first prime coat to a variety of products. The advantages of the process are its automated character, high level of paint utilization, low level of pollution and high throwing power, *i.e.*, the ability to coat recessed areas of complex metal shapes. Cathodic electrodeposition has assumed major commercial significance due to the avoidance of electrochemical dissolution of metal, the impossibility of electrochemical oxidation of the resin at the substrate and the better corrosion protection. Fundamental aspects of electrodeposition process have been reported by Beck.[1–6] The theory which explains organic film formation and the mechanism of film growth has been developed through many investigations, as reported by Pierce and coworkers.[7,8] The similarity of the growth kinetics of organic coatings and oxide films has been demonstrated.[9,10]

Organic coatings applied to metal surfaces provide corrosion protection by introducing a barrier to ionic transport and electrical conduction, where the sorption and transport of ions and uncharged species (water, oxygen) affect the corrosion behaviour of a polymer/metal system.[11–23] The corrosion protection of metallic substrates by organic coatings depends on many factors: (a) the quality of the coating, *i.e.*, electrical, chemical and mechanical properties of polymers, adhesion of the coating to the substrate, sorption characteristics of the coating and permeability to water, oxygen and ions; (b) the type of substrate and the surface modification; (c) metal/coating interface.[24–31]

2. THE KINETICS AND MECHANISM OF THE CATHODIC ELECTRODEPOSITION PROCESS

2.1. The kinetics and mechanism of organic film growth during the cathodic electrodeposition process

The primary process in the case of cathodic electrodeposition of a water-born organic coating on a metal electrode is hydrogen evolution by H_2O discharge:

$$2H_2O + 2e^- \rightarrow H_2 + 2OH^- \quad (1)$$

followed by electrocoagulation of the resin micelles at the cathode surface by neutralization of positively charged groups in the resin with electrochemically generated OH^- ions. The deposition of a coating will occur when the hydroxyl ion concentration (pH of the system) achieves a critical value:

$$R–NH_3^+ + OH^- \rightarrow R–NH_2 + H_2O \quad (2)$$

Constant voltage experiments carried out at lower voltages enabled the observation of current density changes more accurately than is possible at higher voltages (Fig. 1) and a mathematical model of organic film growth has been proposed.[32] An increase in the applied voltage decreases the time necessary to achieve the maximum value of the current density and gives a larger value for that maximum. At voltages higher than 150 V, a maximum was not observed.

If the film formation and the film growth kinetics are the same for the process at both lower and higher voltages, the current density, j–time, t, relationship

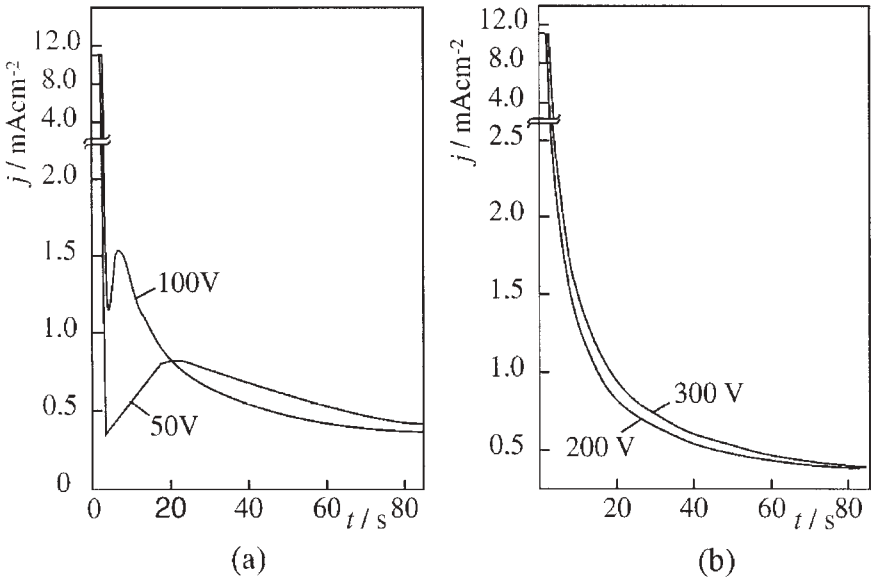

Fig. 1. The current density *vs*. time for the constant voltage electrodeposition of an epoxy coating on steel at lower voltages (a) and higher voltages (b). (From Mišković and Maksimović[32]).

(Fig. 1) can be explained by dividing the process into three steps. The first step is given by Eq. (1) and is represented by an initial plateau of the current density-time curve. The second step is given by Eq. (2) and is represented by a rapid decay of the current density after the initial plateau. In the third step, the electrodeposition process takes place mainly through the porous film, as the surface coverage approaches a value of unity. This step is represented by a maximum of the current density-time curve followed by decrease in the current density. In the third step, reaction (1) takes place in pores. The generated hydroxyl ions react with resin particles outside the pores where transport of resin particles from the bulk ensures a constant resin concentration and a new layer of the polymer film forms. If both reactions (1) and (2) are pseudo-first order reactions, then:

$$\mathrm{A} \xrightarrow{k_1} \mathrm{B} \tag{3}$$

$$\mathrm{B} \xrightarrow{k_2} \text{film} \tag{4}$$

where A is water, B is hydroxyl ion, k_1 and k_2 are the rate constants of the first and the second step of the electrodeposition process, respectively. The usual integration method of kinetics gives:

$$\frac{\mathrm{d}c(\text{film})}{\mathrm{d}t} = \frac{k_1 k_2 c_0(\mathrm{A})}{k_1 - k_2} \left[\exp(-k_2 t) - \exp(-k_1 t)\right] \tag{5}$$

Since the rate of film growth is given by:

$$\frac{\mathrm{d}\delta}{\mathrm{d}t} = \beta(j - j_\mathrm{d}) \tag{6}$$

where δ is the film thickness, β is the coulombic yield and j_d is the dissolution current density, and the film thickness is proportional to the film concentration, c(film), the following relation is obtained:

$$j = K[\exp(-k_2 t) - \exp(-k_1 t)] + j_2 + j_d \quad (7)$$

where $K = k_1 k_2 c_o(A)/(k_1 - k_2)$ is constant and j_2 is the current density on the deposited film.

At lower voltages, where a maximum of the current density-time curve was obtained, if $j_2 + j_d$ = const., the current density in the film pores, j_1, is given by:

$$j_1 = K[\exp(-k_2 t) - \exp(-k_1 t)] >> j_2 + j_d \quad (8)$$

For $dj/dt = 0$, the value of time, t_m, corresponding to the maximum current density in the third step of the electrodeposition process, is given by:

$$t_m = \frac{1}{k_1 - k_2} \ln \frac{k_1}{k_2} \quad (9)$$

The rate constant of chemical reaction of film deposition, k_2, can be evaluated from the experimental current density-time curve for $t >> 0$, using the equation:

$$j = K\exp(-k_2 t) + j_2 + j_d \quad (10)$$

The rate constant of electrochemical reaction of hydroxyl ion evolution, k_1, can be evaluated from the time corresponding to the maximum of the current density-time curve, t_m, and the rate constant k_2 using Eq. (9).

Figure 2 illustrates the agreement between the experimental results and Eq. (7) obtained from the proposed model.[32] The relatively small descrepancy between the calculated and the measured values for low t can be attributed to overlapping between the second and the third steps of the electrodeposition process, *i.e.*, to the impossibility of exact determination of the time when the third step started.

Substituting Eq. (7) in Eq. (6) and integrating, the following film thickness-time relationship was obtained:

$$\delta = \delta_o + \beta K\left[\frac{1 - \exp(-k_2 t)}{k_2} - \frac{1 - \exp(-k_1 t)}{k_1}\right] + \beta j_2 t \quad (11)$$

where δ is the final film thickness and δ_o is the film thickness formed in the second step of the deposition process. The film thickness is plotted versus time for different applied voltages in Fig. 3. The data show that the film grows rapidly at first and then the growth slows but a limiting film thickness was not achieved. For $t >> 0$, the film thickness increases linearly with time, as Eq. (11) shows:

$$\delta = \delta_o + \beta K\left(\frac{1}{k_2} - \frac{1}{k_1}\right) + \beta j_2 t \quad (12)$$

Hence, the presented model of organic film growth[32] proposes a current density-time relationship (Eq. 7) and a film thickness-time relationship (Eq. 11) and en-

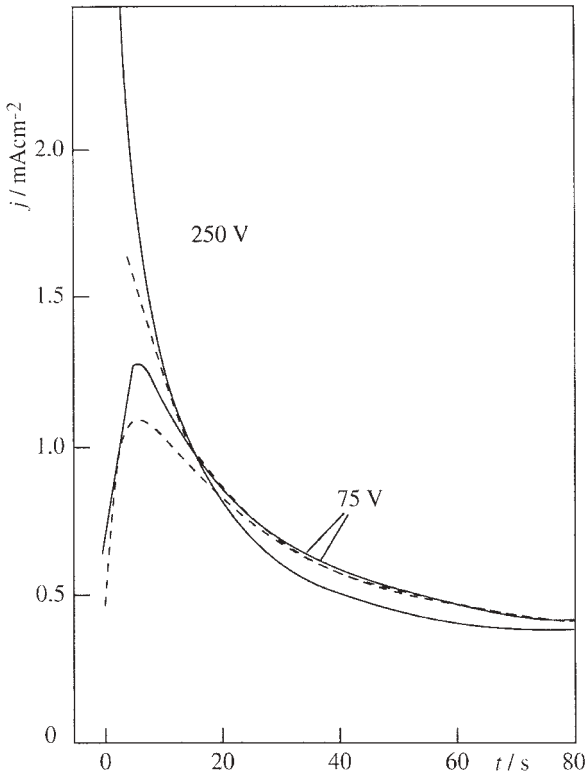

Fig. 2. The current density *vs*. time for the constant voltage electrodeposition of an epoxy coating on steel at 75 V and 250 V: full line – experimental; dashed line – calculated. (From Mišković and Maksimović[32]).

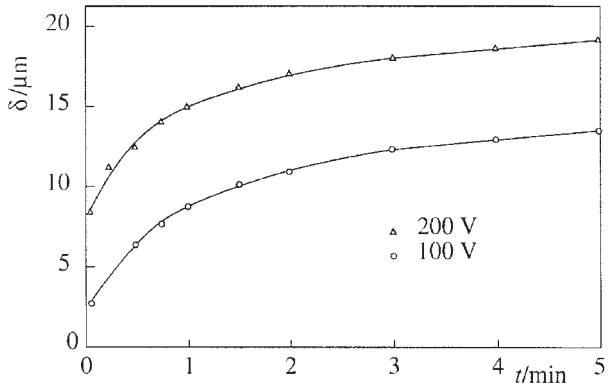

Fig. 3. Increase in the film thickness with time for the constant voltage electrodeposition of an epoxy coating on steel at 100 V and 200 V. (From Mišković and Maksimović[32]).

ables the evaluation of the rate constants for the electrochemical reaction of OH^- ions evolution, k_1, and chemical reaction of film deposition, k_2, which was an unknown procedure in the literature before. The model shows good agreement with experimental results and explains the organic film growth more accurately than the model of Piers,[7] which proposed that a limiting film thickness was achieved. From the dependence of film thickness on the square root of the deposition time[33] (Fig. 4) it can be seen that a linear region which corresponds to the model of Piers exists only at the begining of the

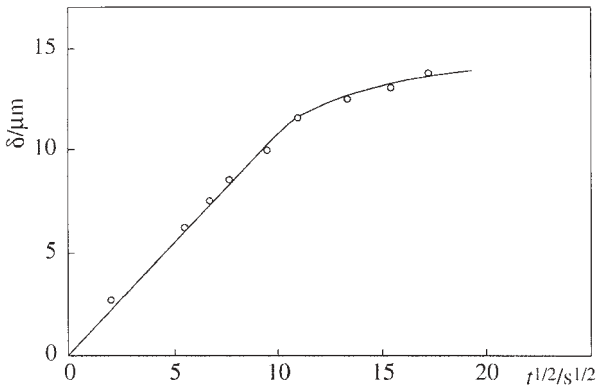

Fig. 4. Dependence of the film thickness on the square root of time for the constant voltage electrodeposition of an epoxy coating on steel at 100 V. (From Mišković-Stanković[33]).

deposition, *i.e.*, for $t^{1/2}<10$ s$^{1/2}$. On the other hand, the model proposed by Mišković and Maksimović[32] is valid over the whole time period, *i.e.*, for both the initial linear region and the subsequent parabolic region. It can be concluded that the proposed model of organic film growth on a cathode corresponds in a large extent to the real cathodic electrodeposition process of an epoxy coating.

2.2. The effect of deposition parameters on the cathodic electrodeposition process

The experimentally obtained dependences of the film thickness, as well as the rate constants k_1 and k_2 on the deposition parameters (applied voltage, resin concentration in the electrodeposition bath and bath temperature)[34-37] can be explained by the proposed model[32] for organic film deposition.

The effect of applied voltage

It was shown[34] that the film thickness increases linearly with applied voltage and that the final film thickness depends on the quantity of electricity in the first step of the deposition process, Q (electrochemical reaction of OH^- ions evolution). From the proposed model, the following relationship between film thickness and applied voltage was obtained:[34]

$$\delta = (\beta a_2 + p + qt) + \beta b_2 U \tag{13}$$

where $p = \beta K(1/k_2 - 1/k_1)$, $q = \beta j_2$, a_2 and b_2 are constants. This relationship corresponds to the experimentally obtained linear dependence between film thickness and applied voltage.

The rate constant of the film deposition reaction, k_2, does not depend on the applied voltage, while the rate constant of the reaction of OH^- ion evolution, k_1, increases exponentially with the applied voltage:[34]

$$k_1 = A_1 \exp(B_1 U) \tag{14}$$

where A_1 and B_1 are constants. The unusually high value for the slope of the curve $\ln k_1$–U of 18 V can be explained by the fact that the hydrogen evolved on the cathode partially blocks the pores of the deposited film, causing the slow diffusion of the hydroxyl ions and a high ohmic overpotential throughout the pores.

The effect of the resin concentration in the electrodeposition bath

It was found[35,36] that the film thickness increases linearly with the resin concentration. From the proposed model,[32] the following relationship between the film thickness and the resin concentration was obtained:[35]

$$\delta = \delta_o + \beta \frac{k_1 k_2 c_0(\mathrm{A})}{k_1 - k_2}\left(\frac{1}{k_2} - \frac{1}{k_1}\right) + \beta j_2 t \tag{15}$$

i.e.,

$$\delta = \delta_o + \beta\, c_o(\mathrm{A}) + \beta j_2 t \tag{16}$$

The results[35] show that the quantity of electricity applied in the first step of the deposition process, Q, the quantity of electricity required to achieve the critical pH for film deposition, Q_o and the thickness of the film formed in the second step of the deposition process, δ_o, are independent of the resin concentration. Hence, Eq. (16) may be rewritten as:

$$\delta = G + \beta j_2 t \tag{17}$$

where $G = \delta_o + \beta c_o(\mathrm{A})$ is constant, which corresponds to the experimentally obtained linear dependence with an intercept on the ordinate axis. Thus, the thickness of the film formed at a fixed deposition voltage increases linearly with the resin concentration and depends only on the current density on the deposited film, j_2.

The rate constant of the film deposition reaction, k_2, increases linearly with the resin concentration,[35] confirming that the deposition of an organic film is a pseudo-first order reaction, as was proposed in the model (Eq. 4).

The effect of the bath temperature

The effect of the bath temperature on the rate constants and the final film thickness has been investigated by the constant voltage method. It was found that the film thickness initially decreases with temperature (at lower temperatures), achieves a minimum value depending on the applied voltage and finally increases (at higher temperatures) and that the final film thickness depends on the quantity of electricity applied in the first step of the deposition process, Q.[37]

The rate constants of the electrochemical reaction of OH^- ion evolution, k_1, and of the chemical reaction of film deposition, k_2, increase exponentially with temperature and Arrhenius activation energies were evaluated.[37] The activation energy of the electrochemical reaction (I step) is about four times higher, 567 kJ/mol, than the activation energy of the chemical reaction (II step), 146 kJ/mol. The unusually high value for the activation energy of the electrochemical reaction can be explained by electroosmosis. Namely, the high energy necessary for water molecules to be squeezed out of the film by electroosmosis depends on the chemical structure of the deposited film, *i.e.*, on the hydrogen bonds between the polymer chains and between water molecules and the polymer chains, on the one hand, and ion-dipole interactions between water molecules and the ends of the emulsion micelles, on the other.

3. THE EFFECT OF THE DEPOSITION PARAMETERS ON THE PROTECTIVE PROPERTIES OF ELECTRODEPOSITED EPOXY COATINGS

Electrochemical impedance spectroscopy (EIS) measurements carried out on epoxy coatings electrodeposited on steel at different values of applied voltage, resin concentration in the electrodeposition bath and bath temperature were used to investigate the effect of deposition parameters on the protective properties of epoxy coating and to determine the deposition parameters resulting in epoxy coatings with the best corrosion stability.[38-43]

The effect of applied voltage

Epoxy coatings electrodeposited at higher voltages (200 V and higher) have larger values of pore resistance, R_p, and smaller values of coating capacitance, C_c and relative permittivity, ε_r, than coatings formed at lower voltages. Changes in the pore resistance, coating capacitance and relative permittivity over time are less explicit for the coatings electrodeposited at higher voltages, which indicates better protective properties and greater stability.[38,39] This behaviour can be explained by the fact that the film thickness increases with applied voltage and that the film thickness determines the corrosion behaviour.[38] The pore resistance, R_p, increases rapidly with applied voltage up to 200 V and then slowly at higher voltages (Fig. 5), so the increase in deposition voltage above 200 V does not significantly affect the protective properties of the epoxy coating.[38]

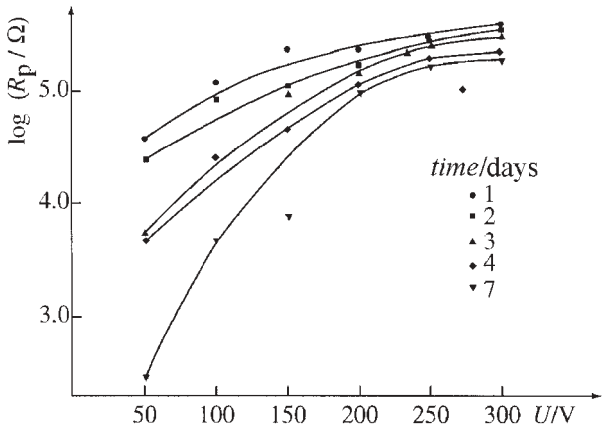

Fig. 5. Pore resistance of epoxy coatings electrodeposited on steel *vs.* applied voltage after different exposure times to 3 % NaCl. (From Dražić and Mišković-Stanković[38]).

The effect of the resin concentration in the electrodeposition bath

Epoxy coatings electrodeposited at higher resin concentration (20 wt.% and higher) have larger values of pore resistance, R_p and smaller values of coating capacitance, C_c and relative permittivity, ε_r, than coatings formed at lower concentraton. Changes in the pore resistance, coating capacitance and relative permittivity over time are less explicit for the coatings electrodeposited at higher resin concentrations, which suggests better protective properties and longer maintenance of the protective properties.[40-43] This behaviour can be explained by the fact that the film thickness increases with resin concentration and that the film thickness determines the corrosion stability.[40]

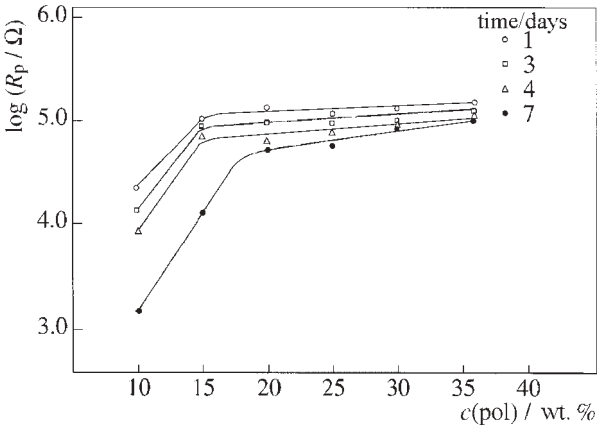

Fig. 6. Pore resistance of epoxy coatings electrodeposited on steel as a function of resin concentration in the electrodeposition bath after different exposure times in 3 % NaCl. (From Mišković-Stanković and Dražić[41]).

The pore resistance, R_p, increases rapidly with resin concentration up to 15 wt.% and then slowly at higher resin concentrations (Fig. 6). This means that the protective properties of coatings formed at resin concentration higher than 15 wt.% do not increase significantly but, on the other hand, the rupture voltage as an undesirable effect appears at lower voltages as the resin concentration increases. Hence, the resin concentration in the electrodeposition bath for epoxy coatings should be about 15 wt. %.[41]

The effect of the bath temperature

Epoxy coatings electrodeposited at higher bath temperatures (27 ºC and higher) have larger values of pore resistance, R_p and smaller values of coating capacitance, C_c, and relative permittivity, ε_r, than coatings formed at lower temperatures.[40,41] Changes in the pore resistance, coating capacitance and relative permittivity over time are less explicit for the coatings electrodeposited at higher temperatures, which indicates better protective properties and longer maintenance of the protective properties. This behaviour can be explained by the fact that the film thickness determines the corrosion behaviour[40] and that the film thickness increases at higher bath temperatures from a minimum value. The pore resistance, R_p (Fig. 7) first decreases with temperature (at lower temperatures), achieves a minimum value at the same temperature at which film thick-

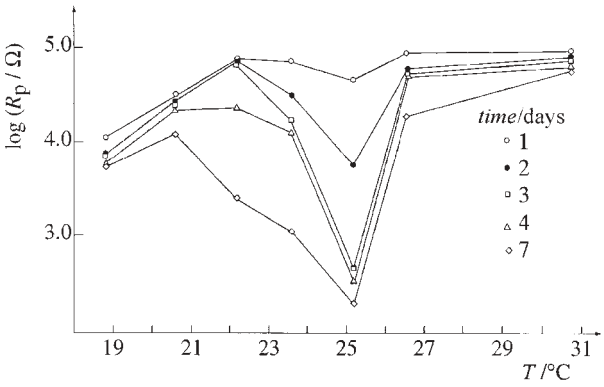

Fig. 7. Plots of the pore resistance of epoxy coatings electrodeposited on steel *vs.* bath temperature after different exposure times to 3 % NaCl. (From Mišković-Stanković and Dražić[41]).

ness attains a minimum value and then increases (at higher temperatures). On the other hand, the increase in bath temperature above 27 ºC does not affect significantly the protective properties of the epoxy coatings but could change the stability of the electrodeposition bath.[41]

4. THE MECHANISM OF CORROSION PROTECTION BY ELECTRODEPOSITED EPOXY COATINGS

From the impedance plots in the complex plane, using the equivalent electrical circuit for polymer-coated metal (Fig. 8, where R_Ω is the resistance of electrolyte and Z_f is the impedance related to the Faradaic reaction at the metal/solution interface) and the fitting procedure elaborated by Boukamp,[44] the time dependences of the pore resistance, R_p and coating capacitance, C_c, were obtained[45,46] (Figs. 9 and 10)

The relative permittivity, ε_r, of the epoxy coating was calculated[45,46] from the film thickness, δ, and the coating capacitance, C_c, using equation:

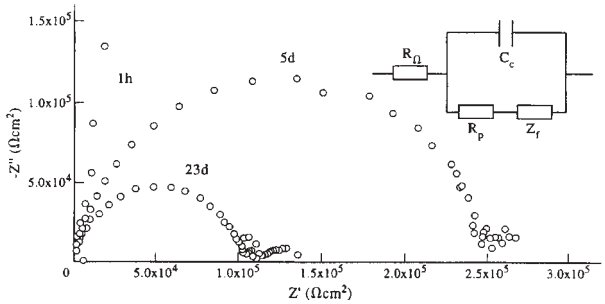

Fig. 8. Complex plane plots for an epoxy coating electrodeposited on steel after various exposure times in 3 % NaCl and the equivalent electrical circuit of a polymer-coated metal. (From Mišković-Stanković *et al.*[45]).

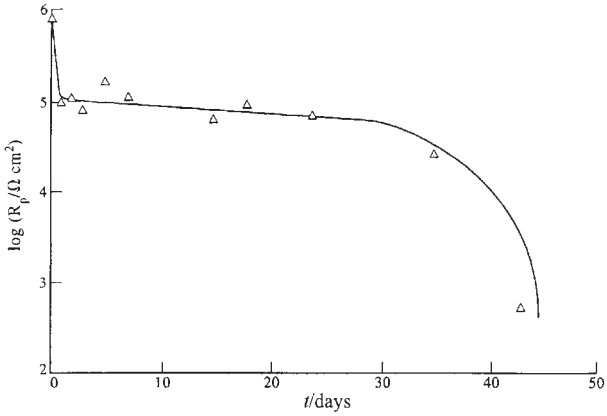

Fig. 9. The time dependence of the pore resistance for an epoxy coating electrodeposited on steel during exposure to 3 % NaCl. (From Mišković-Stanković and Dražić[46]).

$$\varepsilon_r = \frac{C_c \delta}{\varepsilon_0} \tag{18}$$

where $\varepsilon_o = 8.85\times10^{-12}$ F m^{-1}, the permittivity of the vacuum. The time dependence of the relative permittivity of an epoxy coating is presented in Fig. 11. Three time domains may be distinguished in Figs. 9–11, indicating different steps of electrolyte penetration through the coating. The initial decrease in pore resistance (Fig. 9), which coincides

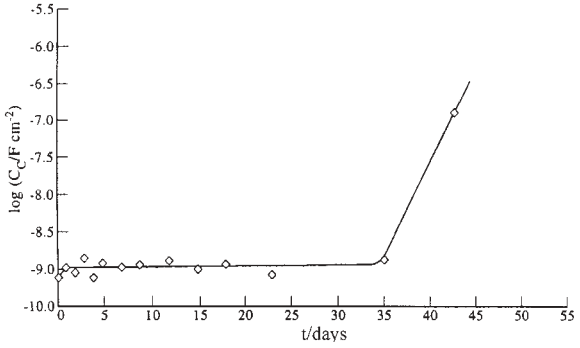

Fig. 10. The time dependence of the coating capacitance for an epoxy coating electrodeposited on steel during exposure to 3 % NaCl. (From Mišković-Stanković and Dražić[46]).

with the initial increase in the coating capacitance (Fig. 10) and relative permittivity (Fig. 11), denotes the entry of electrolyte into the coating.[24,26,47,48] In the second domain, the coating is already saturated with electrolyte and the values of the coating capacitance and relative permittivity are constant over a longer time period, coinciding with plateau in the log $R_p - t$ plot. Finally, there is a rapid change in C_c and ε_r over the third time domain where an increase in the coating capacitance and relative permittivity after a longer period means the beginning of detachment of the coating from the substrate due to loss of adhesion and the start of underfilm corrosion reactions. This period corresponds to final drop of the pore resistance.

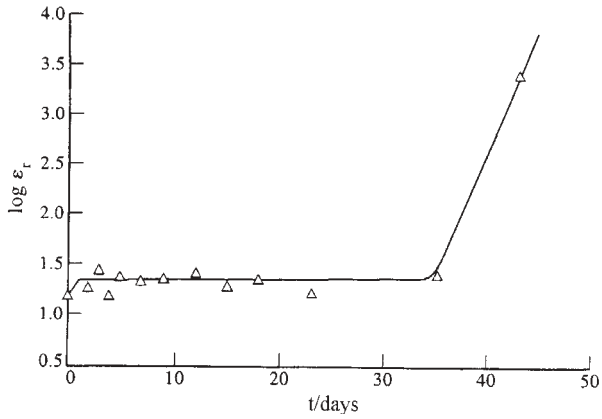

Fig. 11. The time dependence of the relative permittivity for an epoxy coating electrodeposited on steel during exposure to 3 % NaCl. (From Mišković-Stanković and Dražić[46]).

Themogravimetric analysis (TGA) of epoxy coatings exposed to 3% NaCl for various times enabled the integral quantity of electrolyte inside the coating to be determined.[49] From TG curves in the temperature range of 20 ºC to 120 ºC (Fig. 12, where w is the actual mass of coating, w_o is the initial mass of coating and w_f is the mass of coating residue at 600 ºC) and from the mass loss of samples in the low temperature region, the amount of electrolyte that penetrated into the coating during the corrosion process can be calculated. The content of electrolyte inside the coating with time (Fig. 13) shows an initial increase during the first few days, followed by a plateau with a very slow increase and finally a sharp rise after longer immersion time. These results are in good agreement with changes in the pore resistance (Fig. 9), coating capacitance (Fig. 10) and relative permittivity (Fig. 11) with time.

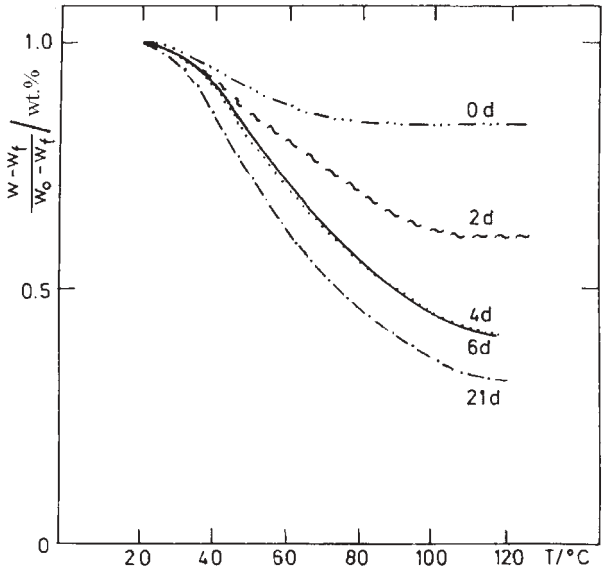

Fig. 12. TG curves of an epoxy coating electrodeposited on steel after various exposure times to 3 % NaCl. (From Mišković-Stanković *et al.*[49]).

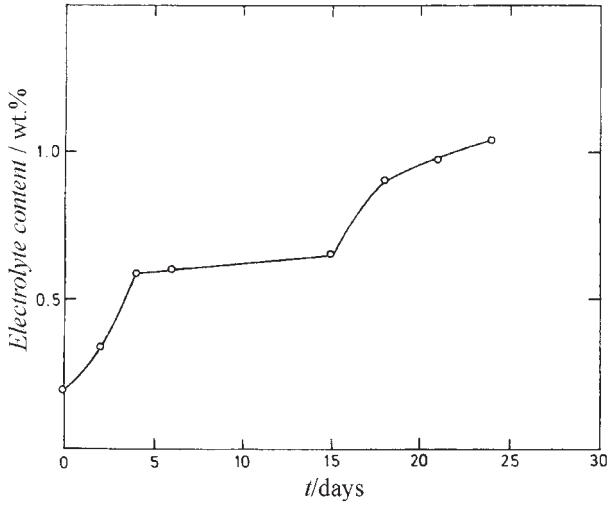

Fig. 13. Increase in the electrolyte content inside an epoxy coating with time of exposure to 3% NaCl. (From Mišković-Stanković *et al.*[49]).

Gravimetric liquid sorption experiments were conducted[45,46] to investigate the mechanism of electrolyte penetration through an epoxy coating and to explain the three time domains observed for the time dependencies of pore resistance, coating capacitance, relative permittivity and electrolyte content inside the coating, since it is known that the first domain depends on the sorption characteristics of the coating. Initially, distilled water was used as the corrosive agent. The gravimetric sorption liquid data are reported as a plot of the amount of water absorbed at time t, m_t, against $t^{1/2}$ (Fig. 14a, sorption curve). The water uptake is linear with $t^{1/2}$ until a steady-state is reached. The observed initial linear behaviour suggests that the sorption is controled by Fickian diffusion. Assuming Fickian behaviour with a constant diffusion coefficient D, the sorption data should obey the equation:[50]

$$\frac{m_t}{m_\infty} = 1 - \frac{8}{\pi^2} \sum_{n=0}^{\infty} \frac{1}{(2n+1)^2} \exp\left[-\frac{D(2n+1)^2 \pi^2}{\delta^2} t \right] \tag{19}$$

where m_∞ is the amount of absorbed water at equilibrium and δ is the film thickness. By series expansion of Eq. (19) for small values of t, one obtains:

$$\frac{m_t}{m_\infty} = \frac{4D^{1/2}}{\delta \pi^{1/2}} t^{1/2} \tag{20}$$

Using Eq. (20), the ratio m_t/m_∞ was plotted against $t^{1/2}/\delta$ (Fig. 14b, reduced sorption curve) and from the initial slope of the linear region, the diffusion coefficient for water across a nonpigmented epoxy coating was calculated[45] to be 3.16×10^{-11}

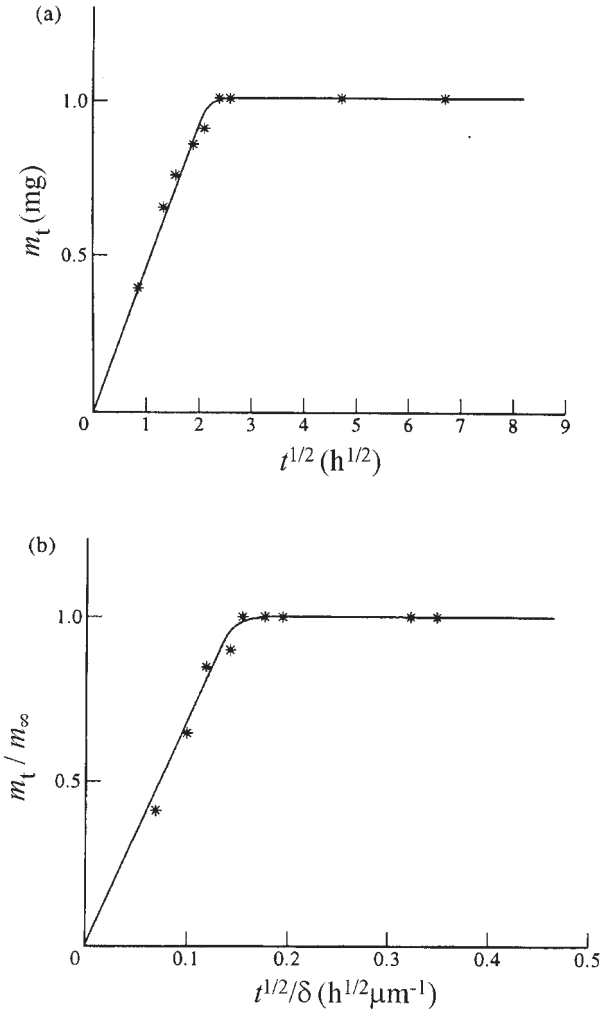

Fig. 14. A plot of the amount of absorbed water at time t, m_t, against the square root of time (a) and the reduced sorption curve (b), at 25 ºC for an epoxy coating during exposure to distilled H_2O. (From Mišković-Stanković *et al.*[45]).

$cm^2\ s^{-1}$. The diffusion coefficient of Cl^- ions across an epoxy coating has been reported[51] as $4.7\times10^{-12}\ cm^2\ s^{-1}$, *i.e.*, one order of magnitude smaller then the diffusion coefficient of water. This suggests that the first step in electrolyte penetration through the coating is related to water uptake in the micropores of the polymer net, which occurs according to Fick's law.[45]

In order to confirm this assumption, gravimetric liquid sorption experiments in the different corrosive agents (3 % NaCl, 3 % Na_2SO_4, 3 % sodium salt of 2-naphthol-3,6-disulfonic acid) were performed.[45,46,52] From obtained sorption curves it can be observed that the time required to saturate the coating with different electrolytes was the same as for saturation with pure water, *i.e.*, independent of the type and dimensions of the ions in the electrolyte (Cl^-, SO_4^{2-}, $C_{10}H_{13}OH(SO_3)_2^{2-}$). From the reduced sorption curves at different temperatures, the values of the diffusion coefficient for water, $D(H_2O)$, and the activation energy of water diffusion through the epoxy coating, E_a, during exposure to different corrosive agents were determined (Table I).[45,46]

TABLE I. The values of the diffusion coefficient for water, $D(H_2O)$, at 25 °C and the activation energy of water diffusion across an epoxy coating, E_a, in different corrosive agents

Electrolyte	H_2O	3 % NaCl	3 % Na_2SO_4	3 % Na salt of 2-naphthol-3,6-disulfonic acid
$D(H_2O)\times10^{11}/cm^2\ s^{-1}$	3.16	2.83	3.85	3.85
E_a/kJ mol^{-1}	14.3	12.0	12.5	13.7

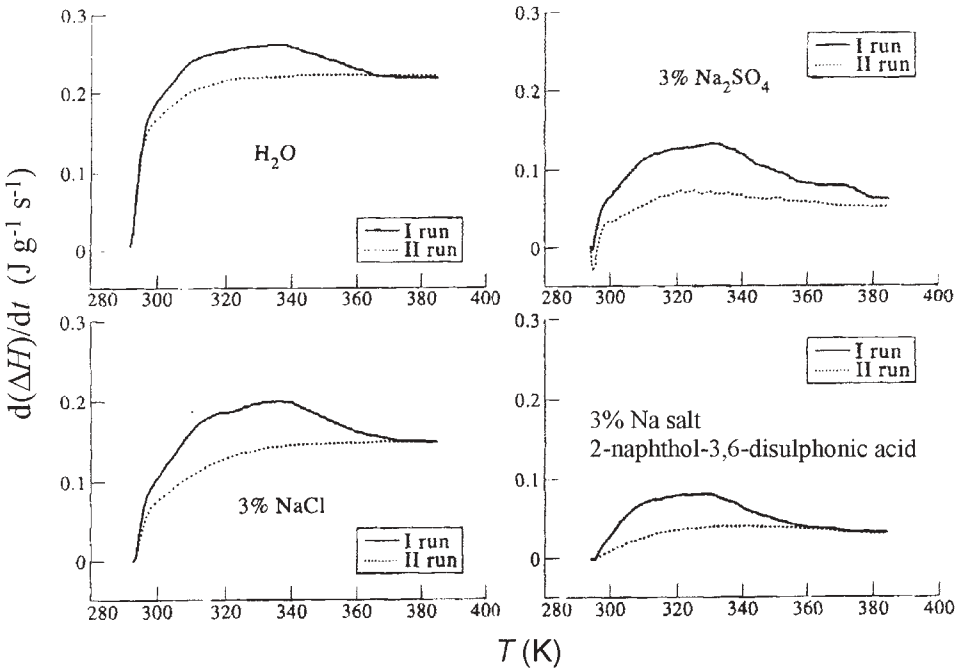

Fig. 15. DSC thermograms for an epoxy coating electrodeposited on steel after 7 days of exposure to various corrosive agents. (From Mišković-Stanković *et al.*[45]).

The very similar values of the diffusion coefficient for water and for the activation energy of water diffusion through the epoxy coating obtained with different corrosive agents, confirm the proposed model of electrolyte penetration,[45,46,52] in which the first step is related to water uptake when molecules of pure water diffuse into the micropores of the polymer net according to Fick's law and is independent of the type and dimensions of the ions present in the electrolyte.

Differential scanning calorimetry (DSC) was used to measure the enthalpy of vaporization of the volatile electrolyte as a function of increasing temperature (between 18 ºC and 110 ºC).[45,46] From the DSC thermograms obtained for the epoxy coating after exposure to the various corrosive agents (Fig. 15), the enthalpies of vaporization of different volatile electrolytes were calculated from the area under the endothermic trace (Table II). From the obtained values of enthalpy of vaporization, the quantity of water inside the coating was calculated for the different corrosive agents (Table II), knowing the average value of the enthalpy of vaporization of pure water between 20 ºC and 110 ºC.

TABLE II. The values of the enthalpy of vaporization, $\Delta_{vap}H$ and the water content inside a coating during exposure to different corrosive agents

Electrolyte	$\Delta_{vap}H$/J g^{-1}	Water content/wt.%
H_2O	18.8	0.80
3 % NaCl	23.3	1.0
3 % Na_2SO_4	24.7	1.1
3 % Na salt of 2-naphthol-3,6-disulfonic acid	21.8	0.93

The similarity of the values of enthalpy of vaporization of the different volatile electrolytes and of the quantity of water inside the coating provides additional confirmation for the first step of the proposed mechanism of electrolyte penetration through an epoxy coating.

The second step of electrolyte penetration, which corresponds to the plateau in the log R_p – t (Fig. 9), log C_c – t (Fig. 10), log ε_r – t (Fig. 11) and electrolyte content – t (Fig. 13) plots, is related to the penetration of water and ions through the macropores which, with time, become deeper and finally penetrate the coating.[45,46,49] The number,dimensions and shape of the macropores through the coating were determined by optical microscopy examination coupled with an image analysis of different coating layers in respect to its depth[49,52] (Fig. 16a). Optical microscopy examination coupled with image analysis enabled the statistical analysis of the micrograph in terms of macropore number, N, pore size distribution, mean pore diameter, r_p, mean pore area, A_p and mean percentage values of the surface covered by pores (Table III).

These data suggest that the mean pore area of the deeper-lying layers is smaller than that of the upper layers inside the coating and that a mean pore should have the shape and dimensions as presented in Fig. 16b. The larger mean pore area at the metal surface with respect to the mean pore area through the last layer indicates the spread of electrolyte under the coating, which causes detachment (delamination) of the coating and corrosion of the metal surface. This is in good agreement with the final rise of the

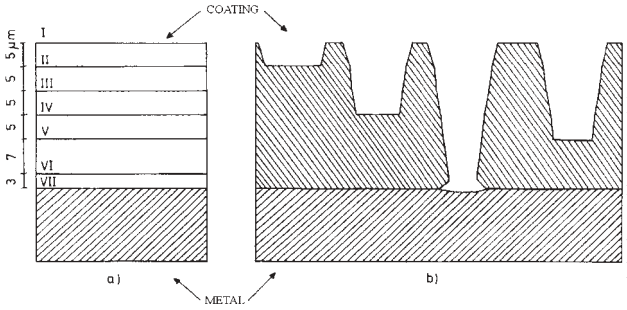

Fig. 16. A schematic presentation of the different layers of a coating (a) and a model of the conducting macropores through a coating as a consequence of electrolyte penetration (b). (From Mišković-Stanković *et al.*[49]).

electrolyte content inside the coating (Fig. 13) obtained by TGA and the increase in C_c (Fig. 10) and ε_r (Fig. 11) after the plateau, obtained by impedance measurements.

TABLE III. The pore number, N, mean pore area, A_p, mean pore radius, r_p and mean percentage of surface covered by pores for each level and its thickness, δ

Layer	δ/μm	N	A_p/μm^2	% of surface covered by pores	r_p/μm
I	30	94	165	6.65	7.2
II	25	34	109	1.61	5.9
III	20	33	104	1.49	5.8
IV	15	30	65	0.85	4.5
V	10	11	53	0.25	4.1
VI	3	10	30	0.13	3.1
Pores through the last layer		4	29	0.05	3.0
Metal substrate		4	85	0.14	5.2

Using the experimental data on the dimensions and shape of the pores through the coating and knowing the number of pores for each layer, the quantity of electrolyte in the conducting macropores was calculated to be 8.4×10^{-8} g.[49] On the other hand, TGA indicated that the integral quantity of electrolyte inside the coating was 5.5×10^{-5} g or 2.3 wt.% of the sample.[49] This means that 0.1 wt.% of the electrolyte (*i.e.*, of total 2.3 wt.%) was located in the conducting macropores and the rest of the electrolyte was situated inside the micropores of the polymer net, causing swelling of the polymer. This also means that the quantity of electrolyte inside the micropores of the polymer net is about one order of magnitude greater than that inside the conducting macropores. Using the following procedure,[49] it was shown that the electrolyte inside the micropores of the polymer net does not affect the overall conduction through the coating, since it appears that practically it depends only on conduction through the macropores. One can calculate the value of pore resistance, R_p, based on non-electrochemical data, *i.e.*, on optical microscopy examination using the equations:

$$\frac{1}{R_p} = \sum_{i=1}^{6} \frac{1}{R_{p,i}} \tag{21}$$

and

$$R_{p,i} = \frac{\rho \delta_i}{P_i} \tag{22}$$

where $R_{p,i}$ is the pore resistance of each layer through the coating (Fig. 16), ρ is the resistivity of the bulk electrolyte (22.8 Ω cm for 3 % NaCl), δ_i is the thickness of each successive layer filled with electrolyte and P_i is area of that layer calculated from the equation:

$$P_i = p_i N_i \tag{23}$$

where p_i is the specific mean pore area obtained by dividing the mean pore area of each layer, A_p, with the pore number of each layer (Table III) and N_i is the number of pores penetrating from the coating surface through the coating to the metal. The results are presented in Table IV.

TABLE IV. Calculated values of the pore resistance based on optical microscopy examination for all pores penetrating to defined depths

Pore penetrated through layers	δ_i/μm	p_i/μm^2	N_i	P_i/μm^2	$R_{p,i}\times10^{-4}$/Ω	$R_{p,total}\times10^{-4}$/Ω*
I,II	5	1.75	32	56.2	2.0	
I,II,III	10	3.20	1	3.2	71.3	
I,II,III,IV	15	3.15	3	9.5	36.0	
I,II,III,IV,V	20	2.16	19	41.2	11.1	
I,II,III,IV,V,VI	27	4.82	1	4.8	128	
To metal	30	3	4	12	57.0	1.53

*Calculated using all $R_{p,i}$ values and eq. (21).

Finally, the expected value of the macropore resistance based on optical microscopy examination using Eq. (21) was calculated to be 1.53×10^4 Ω. Comparing this calculated value with the experimental value obtained from impedance measurements after the same time of immersion, 1.78×10^4 Ω, it can be concluded that the conduction through a coating depends only on the conduction through the macropores and that the overall pore resistance represents the resistance of the macropores which penetrate through the coating. It seems that the electrolyte located inside the micropores of a polymer net does not affect the conduction through the coating although its quantity is by one order of magnitude larger than that in the macropores. This can be explained by the fact that the electrolyte located in the micropores of a polymer net causes swelling of the polymer but does not affect the conduction through coating, because the polymer chains hinder the mobility of ions and water molecules.

In the third step of electrolyte penetration, the macropores penetrate through the coating, which leads to contact between the electrolyte and the metal surface and to the beginning of electrochemical processes at the metallic interface, as can be concluded from the final drop in the pore resistance (Fig. 9) and the final increase in the coating capacitance (Fig. 10), relative permittivity (Fig. 11) and electrolyte content inside the coating (Fig. 13).

5. CONCLUSION

The proposed model of organic film growth on a cathode during the process of electrodeposition corresponds to a great extent to the real process of cathodic electrodeposition of an epoxy coating on steel and shows good agreement with the experimental results. The model, which proposes the current density-time and film thickness-time relationships, enables the evaluation of the rate constants for the electrochemical reaction of OH^- ion evolution and for the chemical reaction of organic film deposition. The dependences of the film thickness and rate constants on applied voltage, bath temperature and resin concentration in the electrodeposition bath have also been obtained.

The deposition parameters have a great effect on the cathodic electrodeposition process and the protective properties of electrodeposited coatings. Epoxy coatings formed at higher voltages, higher bath temperatures and higher resin concentrations have larger values of pore resistance and lower values of the capacitance and relative permittivity of the coating. The changes of these values with exposure time are less explicit for these coatings indicating their greater corrosion stability. Increasing the applied voltage, bath temperature and resin concentration above optimal values has no effect on the protective properties of the coating.

Using EIS, TGA, gravimetric liquid sorption experiments, DSC and optical microscopy, the corrosion stability of the epoxy coatings was investigated. It is suggested that electrolyte penetration through an organic coating occurs in two steps. The first step is related to water uptake, when molecules of pure water diffuse into the micropores of the polymer net according to Fick's law and is independent of the type and dimensions of the ions in the corrosive electrolyte. The second step is related to the penetration of water and ions through the macropores, which leads to contact between the electrolyte and the metal surface and the beginning of electrochemical processes at the metallic interface.

Statistical analysis of the different layers of the coating through its thickness using optical microscopy and image analysis enabled the pore number, pore size distribution, mean pore diameter, mean pore area and mean percentage of the surface covered by pores to be determined. These results suggest the shape and dimensions of the macropores through the coating and, knowing the number of the pores in each layer, the quantity of electrolyte inside the macropores was calculated. It was shown that conduction through the coating depends only on conduction through the macropores, although the quantity of electrolyte in the micropores of the polymer net is about one order of magnitude greater than that inside the conducting macropores.

И З В О Д

МЕХАНИЗАМ КАТАФОРЕТСКОГ ТАЛОЖЕЊА ЕПОКСИДНИХ ПРЕВЛАКА И КОРОЗИОНО ПОНАШАЊЕ ДОБИЈЕНИХ ПРЕВЛАКА

ВЕСНА Б. МИШКОВИЋ-СТАНКОВИЋ

Технолошко-металуршки факултет, Карнегијева 4, п.пр. 3503, 11120 Београд

Претпостављени математички модел раста епоксидне катафоретске превлаке, који даје зависност густине струје од времена таложења и дебљине превлаке од времена таложења, показује добро слагање са експерименталним резултатима и омогућава да

се одреде вредности константе брзине електрохемијске реакције стварања хидроксилних јона и константе брзине хемијске реакције таложења превлаке. На основу тога су изведене зависности дебљине превлаке и константи брзина процеса катафоретског таложења од напона, температуре и концентрације полимера у раствору и показан утицај ових параметара на њих. Заштитна својства катафоретских превлака у великој мери зависе од услова таложења. На основу временских зависности отпорности електролита у порама превлаке, капацитивности и релативне пермитивности превлаке одређених из импедансних мерења, показан је утицај напона таложења, температуре и концентрације полимера у раствору на њена заштитна својства. На основу резултата добијених из спектроскопије електрохемијске импеданције, термогравиметријске анализе, диференцијалне скенирајуће калориметрије, сорпционих мерења и оптичке микроскопије, испитивана је корозиона стабилност полимерних превлака и претпостављен је механизам продирања електролита кроз њих. Такође су одређени облик и димензије проводних макропора и израчунат је садржај електролита у превлаци. Провођење кроз микропоре полимерне мреже је занемарљиво у односу на провођење кроз макропоре иако је количина електролита у њима за ред величине већа у односу на количину електролита у макропорама.

(Примљено 17. јануара 2002)

REFERENCES

1. F. Beck, *Farbe und Lack* **72** (1966) 218
2. F. Beck, *Chem. Ing. Techn.* **40** (1968) 575
3. F. Beck, *Ber. Bunsenges. Phys. Chem.* **72** (1968) 445
4. F. Beck, *Prog. Org. Coat*. **4** (1976) 1
5. F. Beck, in *Comprehensive Treatise of Electrochemistry*, J. O. M. Bockris, B. E. Conway, E. Yeager and R. E. White, Eds., Vol. 2, Plenum Press, New York, 1981, p. 537
6. F. Beck, H. Guder, *Macromol. Chem., Macromol. Symp*. **8** (1987) 285
7. P. E. Pierce, *J. Coat. Technol*. **53** (1981) 52
8. M. Wismer, P. E. Pierce, J. F. Bosso, R. M. Christenson, R. D. Jerabek, R. R. Zwack, *J. Coat. Technol.* **54** (1982) 35
9. Z. Kovac-Kalko, in *Electrodeposition of Coatings*, G. E. F. Brewer, Ed., American Chemical Society, Washington D. C., 1973, p. 149
10. P. E. Pierce, Z. Kovac, C. Higginbotham, *Ind. Eng. Chem. Prod. Res. Dev*. **17**(1978) 317
11. J. E. O. Mayne, *Brit. Corrosion J*. **5** (1970) 106
12. R. E. Touhsaent, H. Leidheiser Jr, *Corrosion* **28** (1972) 435
13. M. W. Kendig, H. Leidheiser Jr, *J. Electrochem*. Soc. **123** (1976) 982
14. L. Beaunier, I. Epelboin, J. C. Lestrade, H. Takenouti, *Surf. Technol.* **4** (1976) 237
15. J. C. Scantlebury, K. N. Ho, *J. Oil Col. Chem. Assoc*. **62** (1979) 89
16. H. Leidheiser, *Prog. Org. Coat*. **7** (1979) 79
17. K. Hladky, L. M. Callow, J. L. Dawson, *Brit. Corrosion J.* **15** (1980) 20
18. F. Mansfeld, *Corrosion* **37** (1981) 301
19. G. W. Walter, *J. Electroanal. Chem.* **118** (1981) 259
20. L. M. Callow, J. C. Scantlebury, *J. Oil Col. Chem. Assoc.* **64** (1981) 140
21. F. Mansfeld, M. W. Kendig, S. Tsai, *Corrosion* **38** (1982) 478
22. M. W. Kendig, F. Mansfeld, S. Tsai, *Corros. Sci.* **23** (1983) 317
23. G. W. Walter, *Corros. Sci.* **26** (1986) 681
24. G. Reinhard, *Prog. Org. Coat*. **18** (1990) 123
25. U. Rammelt, G. Reinhard, *Prog. Org. Coat*. **21** (1992) 205

26. B. N. Popov, M. A. Alwohaibi, R. E. White, *J. Electrochem. Soc.* **140** (1993) 947
27. E. M. Geenen, E. P. M. van Westing, J. H. W. de Wit, *Prog. Org. Coat.* **18** (1990) 295
28. E. P. M. van Westing, G. M. Ferrari, F. M. Geenen, J. H. W. de Wit, *Prog. Org. Coat.* **23** (1993) 89
29. F. Deflorian, L. Fedrizzi, P. L. Bonora, *Corrosion* **50** (1994) 113
30. P. L. Bonora, F. Deflorian, L. Fedrizzi, *Electrochim. Acta* **41** (1996) 1073
31. L. Fedrizzi, F. Deflorian, P. L. Bonora, *Electrochim. Acta* **42** (1997) 969
32. V. B. Mišković, M. D. Maksimović, *Surf. Technol*. **26** (1985) 353
33. V. B. Mišković-Stanković, *Ph. D. Thesis*, Faculty of Technology and Metallurgy, University of Belgrade, Belgrade, 1989
34. M. D. Maksimović, V. B. Mišković-Stanković, N. V. Krstajić, *Surf. Coat. Technol*. **27** (1986) 89
35. V. B. Mišković-Stanković, M. D. Maksimović, *Prog. Org. Coat*. **16** (1988) 255
36. V. B. Mišković-Stanković, M. D. Maksimović, *Zaštita materijala* **32** (1991) 13
37. V. B. Mišković-Stanković, M. D. Maksimović, *J. Serb. Chem. Soc.* **51**(1986) 545
38. D. M. Dražić, V. B. Mišković-Stanković, *Corros. Sci.* **30** (1990) 575
39. M. D. Maksimović, V. B. Mišković-Stanković, *Corros. Sci.* **33** (1992) 271
40. D. M. Dražić, V. B. Mišković-Stanković, *Prog. Org. Coat*. **18** (1990) 253
41. V. B. Mišković-Stanković, D. M. Dražić, *J. Serb. Chem. Soc*. **56** (1991) 343
42. V. B. Mišković-Stanković, M. D. Maksimović, *Bull. Electrochem*. **9**, 2-3 (1993) 69
43. M. D. Maksimović, V. B. Mišković-Stanković, *J. Serb. Chem. Soc.* **59** (1994) 53
44. B. Boukamp, *Sol. St. Ionics* **20** (1986) 31
45. V. B. Mišković-Stanković, D. M. Dražić, Z. Kačarević-Popović, *Corros. Sci*. **38** (1996) 1513
46. V. B. Mišković-Stanković, D. M. Dražić, in *Organic and Inorganic Coatings for Corrosion Prevention*, L. Fedrizzi and P. L. Bonora, Eds., EFC Publications No. **20**, The Institute of Materials, London, 1997, p. 33
47. F. Bellucci, L. Nicodemo, *Corrosion* **49** (1993) 235
48. F. Deflorian, V. B. Mišković-Stanković, P. L. Bonora, L. Fedrizzi, *Corrosion* **50** (1994) 438
49. V. B. Mišković-Stanković, D. M. Dražić, M. J. Teodorović, *Corros. Sci.* **37** (1995) 241
50. J. Crank, *The Mathematics of Diffusion*, Clarendon Press, Oxford, 1970
51. J. Parks, H. Leidheiser, Jr., *Ind. Eng. Chem. Prod. Res. Dev*. **25** (1986) 1
52. V. B. Mišković-Stanković, D. M. Dražić, *Glas CCCLXXX Srpske akademije nauka i umetnosti, Odelj. tehn. nauka* **32** (1996) 67.